Journal of Surgery
Delay A, et al. J Surg 8: 1830
www.doi.org/10.29011/2575-9760.001830
www.gavinpublishers.com
Research Article

Development of Experimental Animal Model and Methodology for Evaluation of a Seroma Prevention Approach

Alexandra Delay[1,2], Julien Vollaire[1], Maxime Henry[1], Anthony Lucas[1], Jean-Luc Coll[1], Véronique Josserand[1] and Georges Bettega[1,3*]

[1]University Grenoble Alpes, INSERM U1209, CNRS UMR5309, Team Cancer Target and Experimental Therapeutics, Institute for Advanced Biosciences F-38000 Grenoble, France

[2]Centre Hospitalier Universitaire Grenoble Alpes, University Grenoble Alpes, F-38000 Grenoble, France

[3]Centre Hospitalier Annecy Genevois, France

[*]**Corresponding author:** Georges Bettega, University Grenoble Alpes, INSERM U1209, CNRS UMR5309, Team Cancer Target and Experimental Therapeutics, Institute for Advanced Biosciences F-38000 Grenoble, France

Citation: Delay A, Vollaire J, Henry M, Lucas A, Coll JL, et al. (2023) Development of Experimental Animal Model and Methodology for Evaluation of A Seroma Prevention Approach. J Surg 8: 1830 DOI: 10.29011/2575-9760.001830

Received Date: 19 June, 2023; **Accepted Date:** 22 June, 2023; **Published Date:** 26 June, 2023

Abstract

Background: seroma is a frequent complication after routine procedures such as mastectomy or latissimus dorsi flap harvesting. Despite multiple attempts to find preventive and curative solutions, seroma remains a major surgical complication. No method of prevention is completely satisfactory at the present time.

Objective: we aim to present an experimental animal model of seroma production after latissimus dorsi muscle and axillary nodes harvest and follow-up protocol to evaluate the efficacy and tolerability of seroma prevention methods.

Methods: we performed a harvest of the right latissimus dorsi muscle and axillary lymph nodes, in 50 Wistar rats divided in 5 groups (n = 10 rats per group). In group I no seroma prevention was performed. Seroma prevention groups were the following: in group II Quilting Sutures (QS), group III Fibrin Glue (FG) application, group IV VENASEAL® application and group V NEXPOWDER® application. Follow-up included standard photographs, in vivo fluorescence imaging of flap perfusion, microCT-scan, seroma puncture and histological flap analysis at POD7, 30 and 90.

Results: we developed a reliable surgical animal model of latissimus dorsi harvest to create seroma as observed in clinical practice. At POD7 the use of QS, FG and VENASEAL® showed a significant decrease in seroma volume compared with control group (respectively $p=0.0016$, $p=0.0005$ and $p<0.0001$) in both microCT-scan and puncture measurements. At POD30 there was no difference between groups. POD7 flap vascularization was significantly lower in control group compared to QS ($p<0.0001$), FG ($p< 0.0001$), VENASEAL® ($p<0.0001$) and non-operated ($p=0.0289$) groups as illustrated by fluorescence imaging. Histological analysis showed significant inflammation in the prevention methods and specifically when a TA was used.

Conclusion: Our animal model and monitoring methodology allow for assessing methods of prevention of seroma as well as the potential associated complications. It may be used as a basic protocol for further studies of innovative tissue adhesives.

Keywords: Flap surgery animal model; ICG-NIR fluorescence imaging; MicroCT seroma imaging; Seroma prevention; Tissue adhesives.

Abbreviations: FG: Fibrin Glue; HES: Hematoxylin Eosin and Saffron; ICG: Indocyanine Green; LDM: Latissimus Dorsi Muscle; NBCA: N-Butyl-Cyanoacrylates Adhesive; NIR: Near Infrared; PBS: Phosphate-Buffered Saline; POD: Postoperative Day; QS: Quilting Sutures; TA: Tissue Adhesives; RLU: Relative Light Units; ROI: Region of Interest.

Introduction

Aggressive oncologic surgical procedures or flap elevations for reconstructive surgery are procedures removing considerable amounts of tissue thus damaging lymphatics and vascular channels and leaving a potential large space. These factors may result in formation of postoperative seroma [1]. Seroma is the most frequent surgical complication after procedures with large tissue elevation such as mastectomy [2], abdominoplasty, [3] or latissimus dorsi flap elevation with a frequency of as much as 79% [4,5]. It increases the risk of flap necrosis, wound infection and delayed wound healing and may cause pain or general patient discomfort [3]. They also often require multiple fluid aspirations and possibly additional surgical procedures thus resulting in socio-economic costs, and possible extended hospital stay. Because of its perioperative morbidity and medico-social consequences, various strategies have been assessed to decrease the incidence of postoperative seroma. Postoperative compression [6], use of closed suction drain [7,8] obliteration of dead space with various flap fixation techniques, use of sclerosants [9,10], talc [11], tranexamic acid [12], fibrin glue and sealants [13-15] associated or not to progressive tension sutures [16] have been attempted with conflicting results and none have been consistent [17] These approaches were generally successful in reducing total seroma output and drainage duration, but not in totally preventing seroma formation [18,19]. To date, no defined protocol nor guidelines exist and surgical prevention technique varies among surgeons. Seroma remains a current clinical issue and may delay adjuvant therapies or impair patients' quality of life. Efforts are still to be made, to find an innovative Tissue Adhesive (TA) that would prevent seroma production. An ideal TA should act as a sealant compressing vascular and lymphatics disrupted vessels and decreasing fluid accumulation. By bonding tissue layers, it may occlude the dead space that would lead to seroma formation, provide strength to the overlying skin flap and promote the flap immobilization thus preventing shearing forces responsible for the inflammatory effect [20,21]. As much as preventing seroma, it should also promote wound healing with an uneventful recovery. Difficulty in TA development lies in the absence of a defined experimental protocol to objectively and comprehensively evaluate a method of seroma prevention. The current models described in the literature focus essentially on the production or not of seroma with iterative punctures, and the evaluation of morbidity is limited to histological analysis [13], [22-26]. Moreover, the animal model mostly described is based on a mastectomy in rats, as described by Lindsey and Harada [22,23]. This model was not reproducible in our hands, due to both frequent reopening of the wounds by the rats themselves and failure to produce seroma consistently. Our aim was thus to develop a reliable experimental animal model as close as possible to the clinical situation and to precise the follow-up protocol to assess the efficacy and tolerance of various seroma prevention methods.

Materials and Methods

Ethics

All animal experiments were performed in accordance with the institutional guidelines of the European Community (EU Directive 2010/63/EU) for the use of experimental animals and were approved by an ethic committee (Cometh38 Grenoble, France) and the French Ministry of Higher Education and Research under the reference: APAFIS#34251-2022020915237986. The present study assessed various seroma prevention methods on 50 rats to which right Latissimus Dorsi Muscle (LDM) and axillary nodes harvest was performed. Fifty female Wistar rats between 280 and 350g were used. Comparison included 5 groups (n = 10 per group) including 3 control groups: group I no seroma prevention (Control Group, CG), group II internal Quilting Sutures (QS), group III fibrin glue (FG) (TISSEEL® of high-thrombin formulation 500 IU thrombin/mL: Baxter Healthcare Corp, Deerfield, IL, USA) - which are the current methods used in practice, and 2 test groups: group IV *VENASEAL®* (Medtronic, Inc, Minneapolis, Minn) and group V NEXPOWDER® (Medtronic, Inc, Minneapolis, Minn).

Surgical Model

All rats were anesthetized with volatile anesthesia. Induction was performed with isoflurane 4% and anesthesia was maintained with isoflurane 2.5%. Each animal was premedicated with a subcutaneous injection of buprenorphine 0.01 mg/kg. The animals were placed in a left lateral decubitus position and the area of interest was shaved, scrubbed with povidone-iodine and locally infiltrated with lidocaine 5 mg/kg. A mediodorsal arched incision was made from the scapular angle to the last thoracic vertebrae. The right Latissimus Dorsi Muscle (LDM) was elevated from its origin along the thoracic and first lumbar vertebrae, up to its humeral insertion. Loose areolar tissue dissection was carried out by peeling the muscle from the subcutaneous tissue, alternating sharp and blunt dissection with fine scissors and gauze pad (Figure 1A). The muscle was individualized on its pedicle (Figure 1B). When identified, the thoracodorsal pedicle was ligated and the

muscle removed. The surface of the harvested muscle was measured in cm^2. Homolateral axillary lymph nodes were removed. Ten subcutaneous scarifications were made on the deep surface of the skin flap to traumatized subcutaneous lymphatic vascularization and increase the risk of seroma (Figure 1C). Meticulous hemostasis was performed by digital pressure or ligation when needed. No electrocoagulation was used. At this point, the procedure varies according to group: no seroma prevention was performed in group I, quilting sutures with 8 stitches of absorbable 4-0 evenly distributed over the entire operated area in group II, application of 1 mL of fibrin glue with pressure of 1 min (group III), application of 8 points of VENASEAL® distributed as the quilting sutures with a pressure of 5 min (group IV), and application of NEXPOWDER® dusted all over the operated area with a pressure of 5 min (group V) (Figure 2). The wound was closed with a double-layer closure (subcutaneous and skin suture) with absorbable 4-0 interrupted suture. Postoperative analgesia was scheduled at 6 hours and 24 hours after surgery using buprenorphine (0.01 mg/kg). All procedures were performed by the same surgeon to prevent operator-dependent conditions. Each operative session included the same number of rats from each group to avoid a learning curve for the operator all along the study. After surgery, rats were housed in individual cages for the first 2 months and then grouped in pairs for the rest of the follow-up.

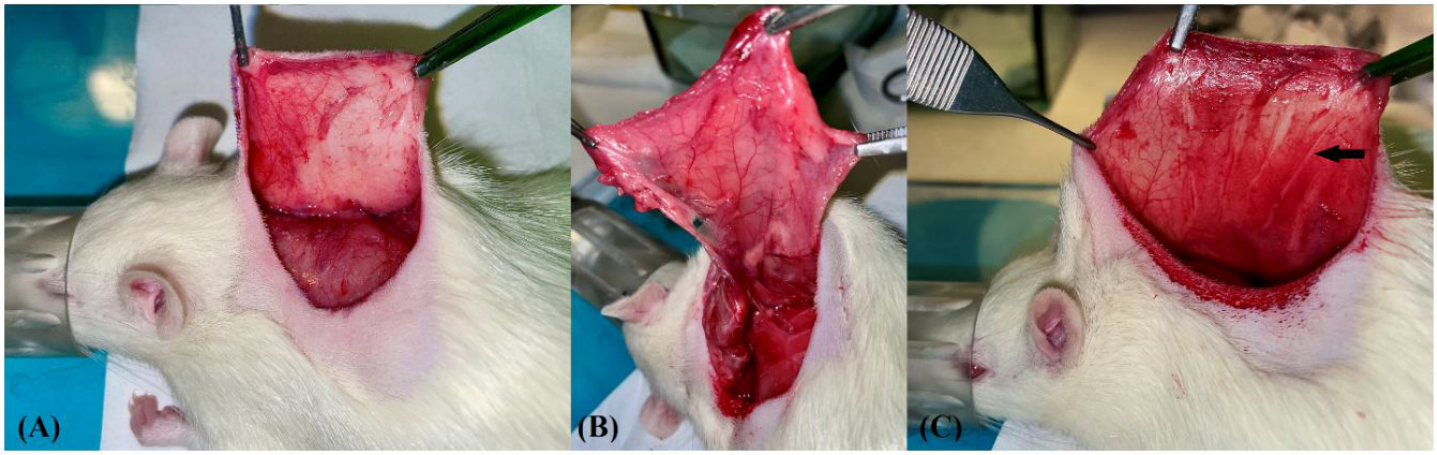

Figure 1: A: Skin flap aspect after peeling the muscle from the subcutaneous tissue. **B**: Exposure of the LDM and the thoracodorsal pedicle. **C**: subcutaneous scarifications made all over the flap. Black arrow points a subcutaneous scarification.

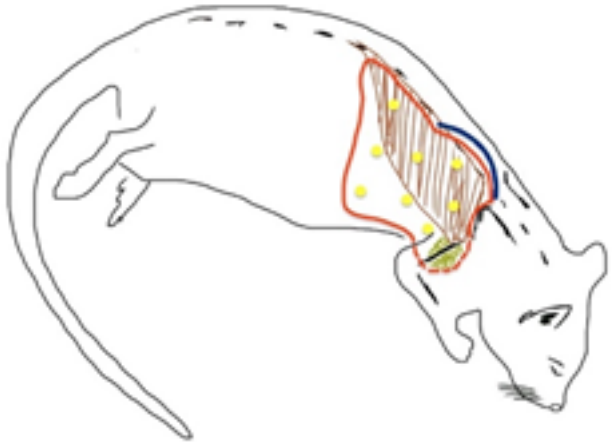

Figure 2: Operative area. Blue line: mediodorsal incision. Red line: surface covered by fibrin glue or NEXPOWDER®. Yellow spots: placement of quilting sutures or VENASEAL® drops.

Experimental Design

Rats were daily exanimated to assess seroma formation, wound infection or opening, flap necrosis, pain or functional impairment. Postoperative follow-up protocol was performed at Postoperative Day (POD) 7, 30 and 90, and included the following stages. All stages were performed under volatile general anesthesia as previously described.

Camera Documentation: Clinical skin assessment was done with standardized photographs taken 20 cm above the animal placed in a left lateral decubitus position so as to see the skin flap entirely. The analysis of the skin flap aspect was based on a skin damages gradation that we made (Table 1). It takes into account both the local inflammatory effect of the therapy used as well as the scratching lesions, related to both the surgery and the means of preventing seroma.

Fluorescence Imaging: Images acquisition was carried out using the Fluobeam® 800 system (Fluoptics, Grenoble, France). The camera was placed at a fixed working distance 15 cm above the rat. An intravenous injection of 400 µL of a 500 mM Indocyanine Green (ICG) solution was performed. Near-Infrared (NIR) fluorescence was recorded in real time from ICG injection over a period of 250 seconds with an image every 2 seconds. The dynamic series of images was then exported and analyzed with the Wasabi!® software (Hamamatsu Photonics, Germany) to quantify the signal intensity. A region of interest (ROI) corresponding to the whole skin flap of the operated site was determined by the examiner. The fluorescence intensity was quantified in relative lights units per 100 milliseconds (RLU/100ms). For each image, the maximum ICG fluorescence value was calculated after subtraction of the background baseline value. All data were compared to the skin fluorescence of five non-operated rats, on the same ROI (future operated skin flap area) to characterize ICG vascular kinetics in normal skin.

Microct-Scan: Seroma volumes were quantified by performing a microCT-scan (vivaCT80, Scanco Medical, Bruttisellen, Switzerland). Images were acquired using a dedicated scan program (energy 45 keV, intensity 114 µA, field of view 79.9 mm diameter, voxel size 100.3 µm, resolution/projection 796/500). If seroma was visually evident or palpable, 1 mL of a contrast agent (iodixanol 320 mg/mL) was injected in the fluid collection with a 29G needle and delicate digital pressure was done to create a clot preventing any fluid extrusion. When no collection was palpable, no injection was performed. The seroma volume was quantified in mm^3.

Puncture: Clinical seroma quantification was performed after the microCT-scan, by draining the fluid collection with an 18G needle. The collected volume was measured in mL. When needed, additive punctures were performed at POD 14 and 21 when the seroma was clinically evident to prevent skin necrosis and potential disabling for the rats. Volumes of these additive punctures were added to the POD30 volume.

Histopathological Analysis: For each group, rats were killed at POD7 (n = 4), POD30 (n = 3) and POD90 (n = 3). Full-thickness biopsies of the skin and chest wall were performed on each side of the animal (operated area, and non-operated side). Biopsies were fixed in 4% buffered formalin for 24h, then rinsed with phosphate-buffered saline (PBS) and put in ethanol 70%. Each fragment was embedded in paraffin and sectioned at 5 µm. standard staining with Hematoxylin Eosin and Saffron (HES) was performed.

Grade I	None	No skin lesion or simple erythema
Grade II	Mild	Skin erosion on < 50% of the surface of the skin flap
Grade III	Moderate	Skin ulceration (superficial skin damage) on < 50% of the surface of the skin flap
Grade IV	Severe	Skin ulceration (superficial skin damage) on ≥ 50% of the surface of the skin flap
Grade V	Necrosis	Presence of skin necrosis (full-thickness skin damage)

Table 1: Skin damages clinical gradation.

Statistical Analysis

Study data were prospectively collected in Microsoft Excel 2016 (Redmond, Washington, USA) and analyzed. All data were analyzed with GraphPad Prism 8 (GraphPad Prism Software Inc., San Diego, CA). Surface of harvested LDM was compared between groups with a one-way ANOVA test to assure group comparability. Seroma volumes were compared using a Kruskal-Wallis test (post hoc Dunn's analysis) for both microCT-scans and punctures. Data are presented as mean ± SEM. Maximum fluorescence intensities of each group were compared with a one-way ANOVA test (post-hoc test: Tukey test). Data are presented as mean ± SEM. Comparison of decreasing intensity signal over time was performed with a two-test ANOVA. Differences were regarded statistically significant when p £ 0.05. Relevant trends were indicated if $p < 0.10$. Statistical analyses were performed for POD7 and POD30 exclusively, as n per group was too small at POD90.

Results

General

No rat presented any movement limitation after surgery nor sign of pain requiring supplementary analgesia or animal sacrifice. The mean surface of the harvested LDM was 19.73 ± 0.53 cm^2 with no significant difference between groups (p=0.1379). No rats developed any allergy to contrast agent nor to any glue. All rats of the NEXPOWDER® group presented a whole flap necrosis with consequent wound dehiscence and large skin defect imposing a sacrifice between POD9 and 13. For ethical matters, we chose to stop this group at n=5. For all the other groups, no rat presented any wound dehiscence or infection, died or developed a problem that required exclusion from the study. One rat presented partial skin flap necrosis in control group and benefited of necrosis excision and closure.

Seroma Formation

All rats of the control group presented seroma formation at POD7 (Figure 3). All fluid collections were serosanguinous in character. At POD7, total seroma volume measured by microCT-scan was 11.7 times lower in QS group (3.15 $x10^3$ ± 0.83 $x10^3$ mm^3), 12.5 times lower in FG group (2.97 $x10^3$ ± 1.09 $x10^3$ mm^3), 27.6 times lower in VENASEAL® group (1.34 $x10^3$ ± 0.90 $x10^3$ mm^3) and 3.3 times lower in NEXPOWDER® group (11.26 $x10^3$ ± 3.58 $x10^3$ mm^3) than in control group (36.99 $x10^3$ ± 5.27 $x10^3$ mm^3). The use of QS, FG and VENASEAL® showed a significant decrease in seroma volume compared with control group (respectively p=0.0016, p=0.0005 and p<0.0001) and no significant difference was found between these 3 prevention groups. There was no significant difference between NEXPOWDER® and control group. At POD7, total seroma volume collected by puncture was 12.1 times lower in QS group (3.24 ± 0.92 mL), 13.4 times lower in FG (2.94 ± 1.13 mL), 23.4 times lower in VENASEAL® group (1.68 ± 0.91 mL) and 3.6 times lower in NEXPOWDER® group (11.00 ± 2.85 mL) than in control group (39.30 ± 5.10 mL). The use of QS, FG and VENASEAL® showed a significant decrease in seroma volume compared with control group (respectively p=0.0017, p=0.0004 and p<0.0001) and no significant difference was found between QS, FG and VENASEAL® groups (Figure 4). There was no significant difference between NEXPOWDER® and control group. No rat of the tests group presented seroma at POD30. However, as we chose to add punctures of POD14 and POD21 to those of POD30, quantification of puncture at POD30 differed from microCTscan measurements. At POD30, total seroma volume collected with puncture was 16.5 times lower in QS group (1.99 ± 1.52 mL), 11.6 times lower in FG group (2.83 ± 2.64 mL), 131.4 times lower in VENASEAL® group (0.25 ± 0.17 mL) than in control group (32.85 ± 14.35 mL). There was no significant difference between groups (Figure 4). There was a relevant trend between control group and VENASEAL® group (p=0.0528). At POD30 total seroma volume on microCT-scan was 13.85 $x10^3$ ± 5.49 $x10^3$ mm^3 in control group; 0.00 mm^3 in every test group. There was a significant difference between control group and each prevention group (p=0.0006 for each). No difference was found between each test group. No rat presented seroma at POD90.

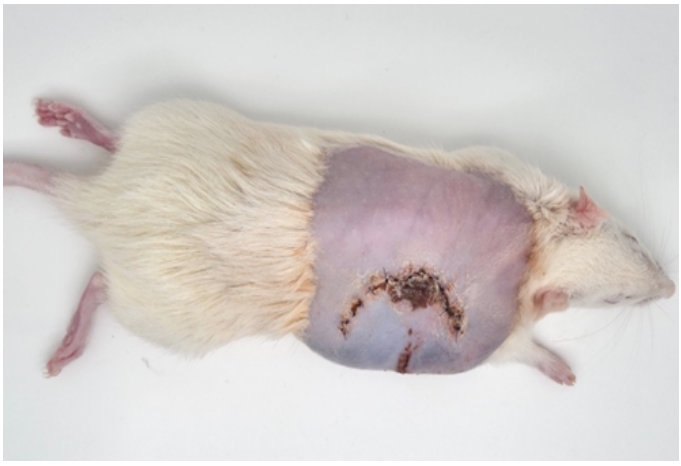

Figure 3: seroma prior to aspiration at POD7.

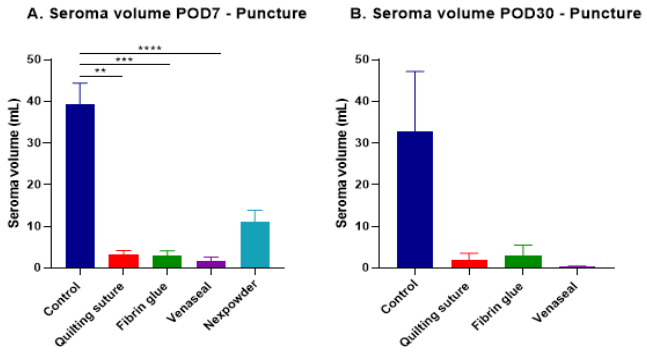

Figure 4: A: Seroma volumes (mean ± SEM) at POD7, in control group (n=10), QS group (n=10), FG group (n = 10), VENASEAL® group (n = 10), and NEXPOWDER® group (n=5). Statistical analysis: * p<0.05; ** p<0.01, *** p<0.001, **** p<0.0001. B: Seroma volumes at POD30 (mean ± SEM; n = 6 animals/group) in control group, QS group, FG group, and VENASEAL® group. Volumes of POD14 and POD21 additive punctures were added to the POD30 volume.

Skin Lesion Gradation

At POD7, rats in control group presented in majority no or mild skin lesions. In the QS group, the predominant skin damage was mild to moderate. In the FG and VENASEAL® groups, skin damages were mostly moderate to severe. 20% of the control group, 10% of the FG group and 20% of the VENASEAL® group

and 100% of the NEXPOWDER® group presented necrosis of the skin flap. At POD30, skin lesions were mainly absent or mild in control and QS groups. It was moderate in FG group. Grades I to IV were found non-homogeneously in the VENASEAL® group. No rat showed skin necrosis. At POD90, skin lesions were absent in the entire control group and predominantly in the QS group. Most of the FG and VENASEAL® groups showed minimal or no skin involvement. One third of the VENASEAL® group still showed moderate involvement.

ICG-NIR Fluorescence Imaging

At POD7, the maximum fluorescence intensity was 48.9 ± 8.4% (control), 151.1 ± 10.4% (QS), 144.1 ± 6.9% (FG), 147.6 ± 10.9% (VENASEAL®) and 60.9 ± 17.0% (NEXPOWDER®) of the one of the non-operated group and these differences were significant for control (p=0.0289), QS (p=0.0289), and VENASEAL® (p=0.0436) groups (Figure 5A). Maximum intensity was 309.2 ± 21.2% (QS), 294.7 ± 14.1% (FG), and 302.1 ± 22.4% (VENASEAL®) and 124.6 ± 34.8% (NEXPOWDER®) of the one of the control group. Maximum fluorescence intensity was highly significantly different between control group and QS (p<0.0001), FG (p<0.0001), and VENASEAL® (p<0.0001) groups. It was significantly different between QS and VENASEAL® groups with non-operated group (p=0.0289 and p=0.0436 respectively). There was a relevant trend but no significant difference between FG and non-operated group (p=0.0841). The fluorescence signal kinetic of the control group was clearly slowed down compared to the one of the non-operated group (p=0.0063) illustrating a longer blood circulation and drainage time. (Figure 6A). Similarly, the NEXPOWDER® group also displayed a slowed down kinetic compared to the non-operated group but not statistically significant (p=0.1851). On the contrary, the fluorescence signal kinetics of QS, FG and VENASEAL® groups were close to the one of non-operated group and were thus very different from the one of the control group (QS: p=0.0007; FG: p<0.0001; VENASEAL®: p<0.0001). There also was a significant difference in signal kinetics between FG and VENASEAL® groups with non-operated group (respectively p=0.0184 and p=0.0011). There was no significant difference between QS group and non-operated group (p=0.3807). At POD30, maximum intensity signal was 79.8 ± 6.2% (control), 144.1 ± 11.3% (QS), 136.2 ± 12.5% (FG) and 149.9 ± 7.9% (VENASEAL®) of the one of the non-operated group but these differences were not significant (Figure 5B). Nevertheless, maximum intensity signal was 180.6 ± 14.1% (QS), 170.7 ± 15.7% (FG) and 187.9 ± 10.0% (VENASEAL®) of the one of the control group. QS, FG and VENASEAL® groups displayed significant differences compared to the control group (p=0.0129, p=0.0467 and p=0.0047 respectively).

At POD30, fluorescence signal kinetics showed a trend toward normalization for control, QS, FG and VENASEAL® groups compared to the non-operated group (Figure 6B).

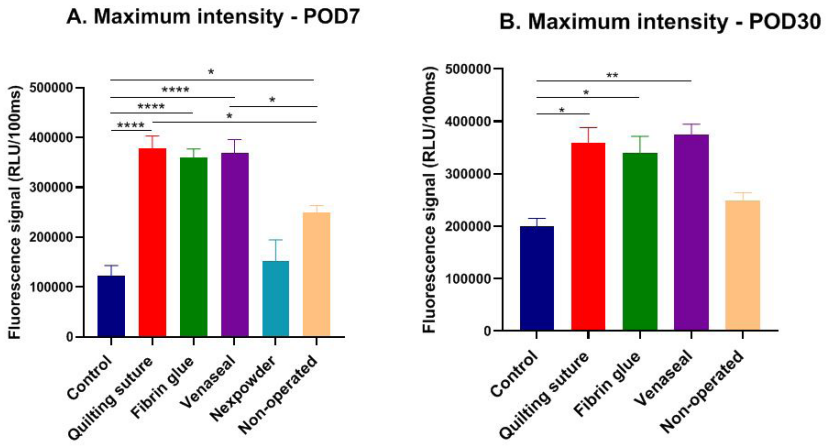

Figure 5: Maximum fluorescence signal intensity after intravenous injection of ICG (mean ± SEM) at POD7, in control group (n=10), QS group (n=10), FG group (n=10), VENASEAL® group (n=10), NEXPOWDER® group (n=5) and non-operated rats (n=5). Statistical analysis: * p<0.05, ** p<0.01, *** p<0.001, **** p<0.0001. Maximum fluorescence signal intensity (mean and SEM) at POD30, in control group (n=6), QS group (n=6), FG group (n=6), VENASEAL® group (n=6) and non-operated rats (n=5). *: significant (p<0.05) difference between indicated groups.

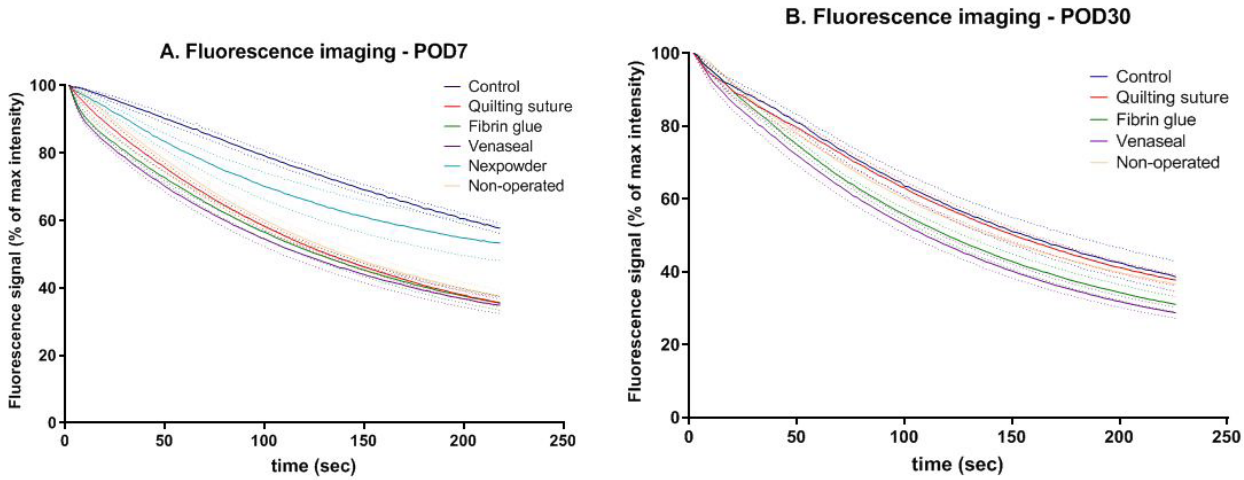

Figure 6: Decreasing percentage of fluorescence signal after intravenous injection of ICG at POD7 (A) in control group (n=10), QS group (n=10), FG group (n=10), VENASEAL® group (n=10), NEXPOWDER® group (n= 5) and non-operated rats (n=5); and at POD30 (B) in control group (n= 6), QS group (n=6), FG group (n= 6), VENASEAL® group (n= 6) and non-operated rats (n=5).

Necropsy

No microorganism, edema, or hemorrhage was detected in any of the samples examined. At POD7, histological analysis showed an inflammatory reaction in control group and the skin flap was completely separated from the chest wall, forming a large dead space with a ragged floor. In contrast, skin flap was firmly adherent to the chest wall when a prevention method was used. Major inflammation was present in FG as much as in VENASEAL® groups, while it appeared to be moderate in QS group. For NEXPOWDER® group, all the tissue layers were subject to severe inflammation and necrosis (Figure 7). Inflammatory cells were mostly fibroblasts, neutrophils and macrophages in all groups. At POD30, inflammatory cell infiltration was milder in control and QS groups. In FG group inflammatory reaction was moderate, while it was severe in VENASEAL® group. The seroma cavity was persistent in control group (Figure 8). At POD90, control and QS groups were no subject to inflammation and tissues were healing well with mild focal fibrosis visible. The appearance of the control group showed a return to normal structures organization, with the flap was adherent to the chest wall. Inflammation persisted and the epidermis was more damaged for FG and VENASEAL® groups (Figure 8).

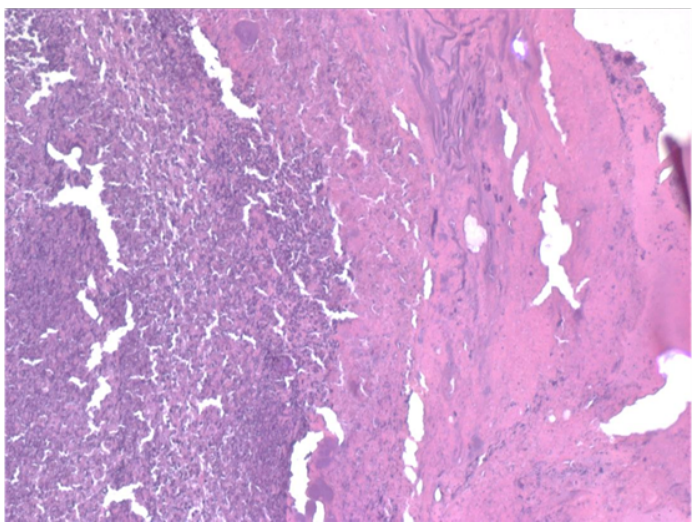

Figure 7: HES-stained tissue in the rat LDM harvest model at original magnification x50 in NEXPOWDER® group illustrating both necrotized zones and severe inflammation.

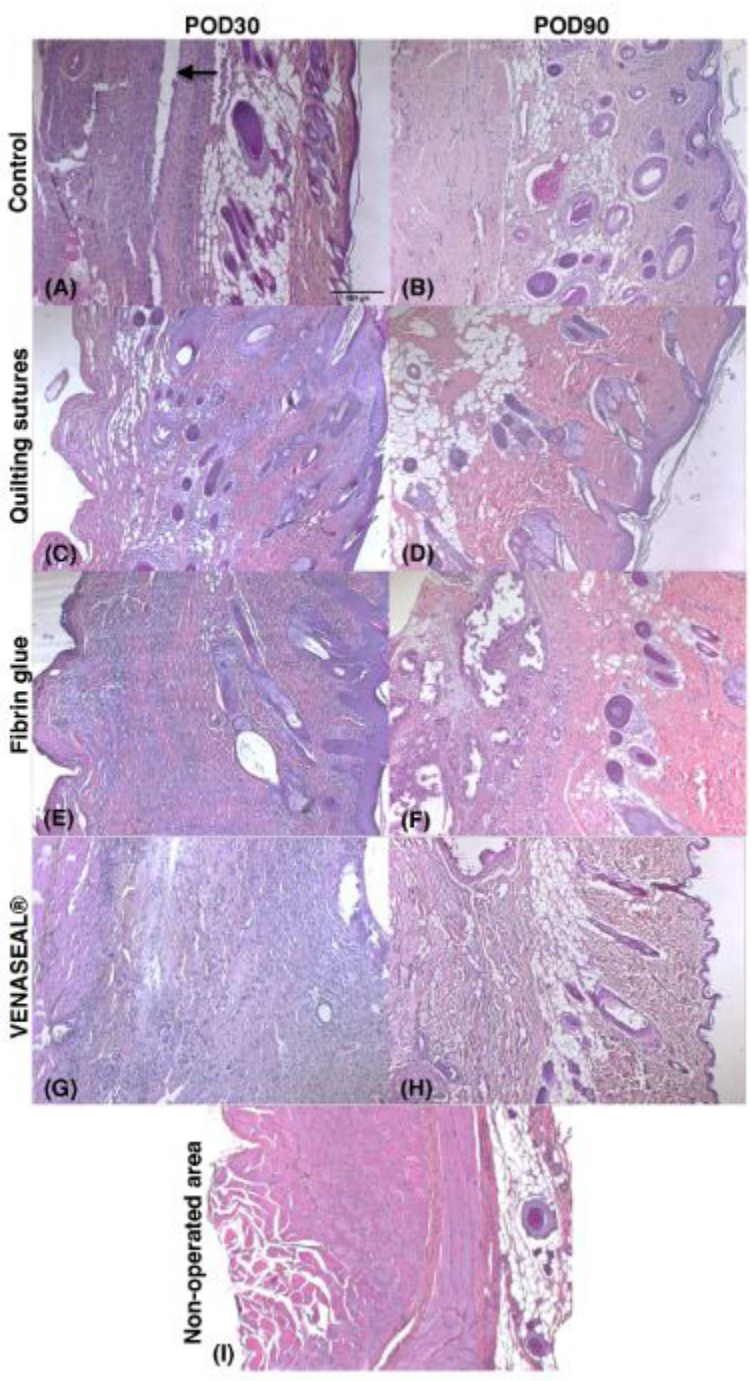

Figure 8: HES-stained tissue in the rat LDM harvest model at original magnification x50. A: control group at POD30 and B: control group at POD90. Black arrow shows the persistent seroma space. C: QS group at POD30 and D: QS group at POD90. E: FG group at POD30 and F: FG group at POD90. G: VENASEAL® group at POD30 and H: VENASEAL® group at POD90. I: healthy tissue from symmetric non-operated area.

Discussion

The objective of our study was to develop a complete and transversal approach for assessment of seroma prevention methods and their possible side effects. The first strong point of our study lies in our reliable animal model. We had initially planned the technique of mastectomy in rats by jugulo-xiphoid incision as described in the literature [22,23] but in our case this model had the major disadvantage of not being reproducible. The scar was easily accessible and could be opened by the rat itself in the first days after surgery, despite a two-layer suture. Although new sutures were performed at each re-opening, we found that seroma production was inconsistent or even almost non-existent in the resutured rats. Given the relatively low incidence of seroma with the mastectomy technique, we chose to carry out a different surgical model. To produce seroma formation, we performed a LDM harvest as inspired from scientific literature [13,26]. Our model associating LDM harvest, removing of axillary nodes and subcutaneous scarifications presents the great advantage of providing reliably seroma as 100% of the operated rats presented seroma in large quantity when no prevention was carried out. This surgical technique is reliable, simply reproducible, with a constant anatomy and an easy approach.

It causes no functional impotence nor significant pain to the rat. Finally, it has the major advantage of a dorsal approach that is inaccessible to rats and therefore not subject to wound opening. The continuation of our work consisted in a methodological development for the follow-up of seroma formation and the monitoring of possible side effects of prevention methods. It has the advantage of being transversal and complete. In the first place, standardized photographs permitted a macroscopic and clinical analysis of the skin flap and we defined a dedicated lesion grading by taking into account the sequalae created by seroma as much as the inflammatory impact of the prevention method used. Then, in order to objectify the clinical examination and to go further with quantified analyses, we associated an exploration of microvascular perfusion by ICG-based NIR fluorescence imaging. ICG is a suitable fluorescent tracer for non-invasive evaluation of cutaneous blood flow and may be used as an index of tissue perfusion [27-29], as it permits to quantify skin perfusion down to a depth of 3 mm [30]. Another key point brought by our methodology is the addition of a CT-scan to the puncture. CT-scans for animals are mainly used for bone density analysis and are not very sensitive to differentiate fluids from soft tissues. A seroma study found in the literature quantified the seroma with CT-scan but their protocol was not detailed enough to be reproducible [31]. After several acquisition attempts at different voxel size, resolution, energy or intensity, and additional subcutaneous injection of PBS (phosphate-buffered saline) on sacrificed rats, we were unable to obtain a reliable quantification of the liquid volume.

The addition of a standard X-ray contrast agent (iodixanol 320 mg/mL) finally permitted to quantify the volume of the seroma in a simple, reliable and efficient way (Figure 9). The reliability of CT quantification might be a tool to assess the natural history of seroma production without the need for iterative punctures. Finally, histopathological analysis concludes the follow-up protocol, as it provides microscopic confirmation of the results obtained from photographic documentation and ICG-NIR fluorescence imaging, regarding potential TA side effects. Our results at POD7 showed a tendency to inflammation and discomfort for the rats in all test groups whereas control group presented relatively lower skin lesions. Necrosis was macroscopically assessed and found both in control group and all TA groups, with a majority in NEXPOWDER® group. This suggests a higher necrosis risk associated with TA or resulting as a sequalae in case of great seroma formation.

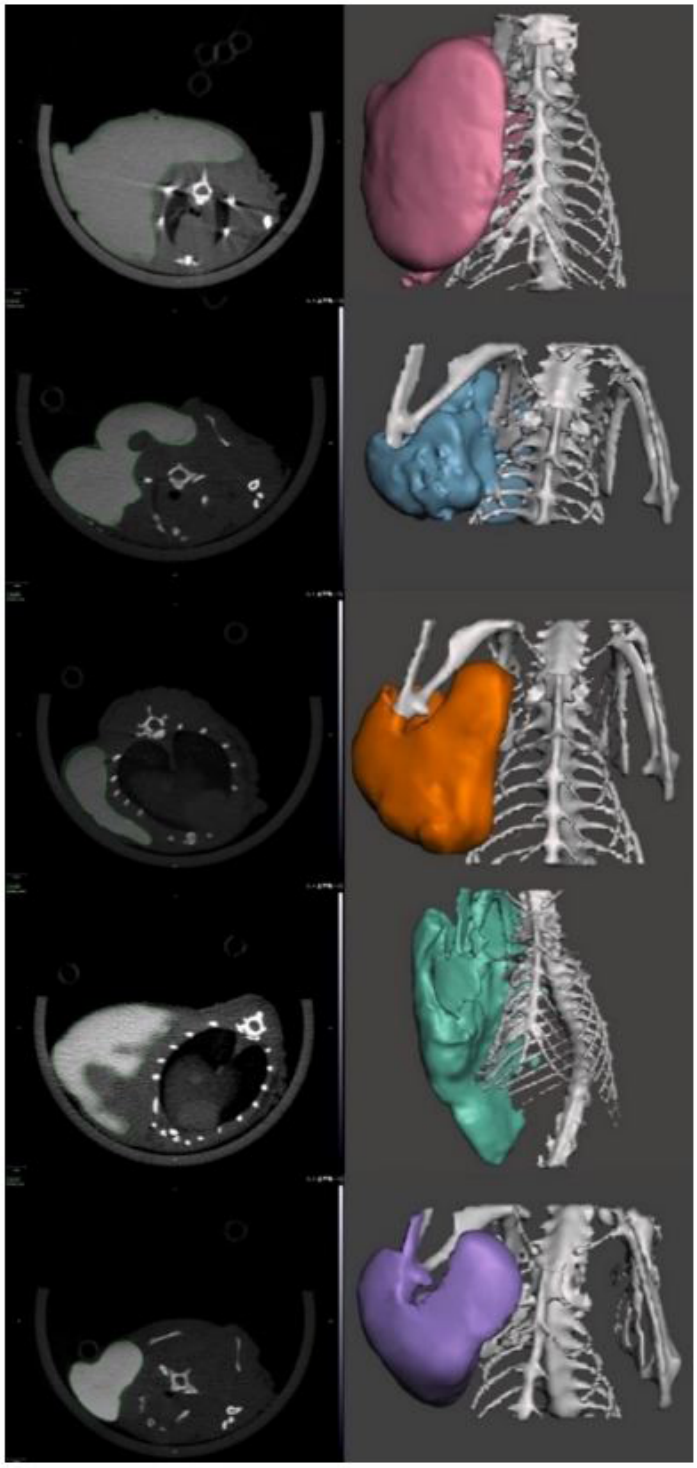

Figure 9: microCT-scan seroma quantification after iodixanol 320 mg/mL injection at POD7. From up to down: control group, QS group, FG group, VENASEAL® group and NEXPOWDER® group.

ICG-NIR fluorescence imaging resulted in different fluorescence signal intensities, revealing inflammation when increased fluorescence signals were measured, as observed at POD7 for QS, FG or VENASEAL® in our study. Inflammation appeared to be related to the use of a TA or absorbable sutures. On the other hand, when fluorescence signal was lowered compared to non-operated group, it revealed skin areas which were altered or would necrotize. In our study, NEXPOWDER® showed a lower signal and decreasing intensity at POD7 and skin flap was macroscopically necrotized a few days after. As for seroma, not only was the fluorescence signal significantly lower than in non-operated rats, but it also decreased more slowly than in non-operated rats, QS, FG and VENASEAL® groups. Seroma is associated with a higher risk of flap necrosis, which is thus easily suggested by ICG-NIR. Hypothesis is that ischemic damages are related to both the damages to vascular supply when elevating the skin flap, and the fluid collection creating a separation between the skin flap from the underneath vascular subcutaneous matrix. Moreover, the soft tissue distension and compression created by seroma may impact venous return, which could explain the slower decrease in fluorescence signal intensity seen on POD7 curves. We hypothesize that NEXPOWDER® showed no different intensity from non-operated rats, as it was a mixture of necrotized area and inflamed area in still living tissues. At POD30, all fluorescence signal kinetics tended to decrease with the same velocity which can be explained by the decrease of seroma volume, wound healing and normalization of inflammation. Clinical superficial skin alterations may not represent the true extent of subcutaneous tissue damage. Our results thus suggest that ICG-NIR imaging is a more reliable method to analyze the whole thickness flap, than clinical analysis only. Signal is decreasing in case of skin ischemia or necrosis, whereas it is increasing with vascular proliferation found in inflammation, compared to normal skin response. Histological analysis confirmed our clinical and imaging results, since we found significant inflammation in the prevention methods and specifically when a TA was used. In the long term, inflammation reaction was reduced in control and QS groups and lasted longer in group FG and VENASEAL®. The combination of photographs, NIR-fluorescence and histological analysis is a relevant and very complete method for characterization of the potential cutaneous side effects of TA. A strong point of the present study lies in the variety of experimental groups, including a control group which was the reference for seroma quantification and its potential sequalae, a non-operated control group which represented the goal to be achieved, two gold standard test groups and two adhesives newly tested in this seroma context. As for test groups, the two referent groups were QS and FG groups, which are the two techniques most employed in practice and which are known to diminish seroma rate [32]. Internal fixation technique with QS according to the "Chippendale" technique [33] is the most performed alternative to TA. It is effective to reduce seroma production [34-36] when adequately and sufficiently distributed over the whole operated area. It has the major advantage of being cheap and relatively easy to perform for an experimented surgeon. The major drawbacks of QS are the additional operative time and potential effect on cosmesis by potentially giving rise to a dimpling effect on the skin, decreasing patient satisfaction and aesthetic outcome [37]. FG is the most commonly used adhesive for wound or internal surgeries, with a large range of clinical and research applications as adhesives, sealants or even drug release matrix. FG acts both as a hemostat and an adhesive. It favors hemostasis and prevents hematomas, while acting as a sealant occluding oozing vessels and filling the dead space. Although many studies defend the effectiveness of FG for seroma prevention [13,15,38], others show that FG does not consistently bring favorable results [14,39-41], especially in large operated areas [42]. FGs are biocompatible and offer TA properties, but present relatively weak tensile and adhesion strength [43,44]. Moreover, FGs can satisfyingly fill the dead spaces, but most probably delay or compromise the re-approximation of the dead spaces by bridging healing tissues when thick layers of glue are used. This may explain why seroma is not completely prevented by fibrin glues when used as dead space fillers or sealant [45].

The other test groups of the present study were two TA that are not presently used in routine for seroma prevention.

VENASEAL® is a N-Butyl-Cyanoacrylate Adhesive (NBCA) of internal use, with various clinical application. NBCAs are widely used for surgeries, particularly for wound repair as alternatives of sutures with rapid setting time (generally less than 5 min) in moist environment. NBCAs have the ability to strongly bond tissues together. However primary concern with cyanoacrylates lies in their histotoxicity, which can result in necrosis, sterile local infection, persistent inflammation and extensive fibrosis [46,47]. More recently, the biocompatibility of NBCAs was underlined by some authors, defending that it should simply be used in small quantities to limit the accumulation of a dissipated heat produced during polymerization and which can induce tissue damage [48]. NBCAs are now used not only for external use but also for various indications such as hernia mesh fixation [49], bone adhesion [50], arterial embolization [51,52] or ablation of varicose veins [53]. As for seroma prevention, NBCAs appear to be effective without significant toxicity according to some recent studies [54,55]. In our case, VENASEAL® was very effective in significantly preventing seroma production, but appeared to be prone to inflammatory reactions over the entire surface of the skin flap, despite being applied in very small quantities and in a dispersed manner. VENASEAL® is a TA with a strong adhesive power, but its use over large areas of detachment might be of high risk of cutaneous toxicity. NEXPOWDER® is a TA based on oxidized dextran and

ε-poly-L-lysine. It is a powder which transforms in an adhesive hydrogel with a Schiff base formation, when getting in contact with tissue moisture [56]. It is commonly used in clinical practice as a hemostat in digestive endoscopy [57-59]. It may also be used as an antiadhesion biomaterial providing deep wound healing while limiting progression of fibrosis [60-62]. It has adhesive and anti-microbial properties while being biocompatible [63]. We chose to use NEXPOWDER® as a hydrogel in apposition between the chest wall and the skin flap, acting like a biomaterial filling the dead space while promoting an anti-fibrotic effect. Its immediate transformation into a gel makes it difficult to distribute evenly over the entire surgical area [64]. In the case of the convexity of the chest wall and axillary fossa, spraying the powder probably created inequitable amount of powder, resulting in accumulation sites. Furthermore, we sprinkled the powder on site after simple washing with PBS, but without adding any additional saline solution. Our main hypothesis is that during the transformation into a gel, the powder created a global drying of the surgical site. All these associated mechanisms might explain why in our case NEXPOWDER® eventually led to skin flap necrosis for all rats. Since seroma prevention did not appear to be particularly effective at POD7 compared with other test groups, and in view of the short-term sacrifice of rats, we chose not to continue this group after the failure of n = 5 rats. As for our study, seroma quantification with both the microCT-scan and puncture, did not permit to elect a prevention method with respect to the other. The use of QS, FG and VENASEAL® all showed a significant difference in seroma volume at POD7 compared with control group but no significant difference was found between any prevention groups. At POD30 or POD90, there was no difference in seroma production between groups.

Conclusion

Seroma is a common and frustrating complication of many surgical procedures. The high incidence of postoperative seroma, its medico-social associated costs and the loss of quality of life for patients have motivated multiple clinical investigations for seroma prevention or minimization. Various methods have been attempted, but none has proven to be entirely effective to date. We developed an animal experimental model and methodology which quantitatively assess seroma production while demonstrating the sequalae of seromas and the side effects of their prevention methods. In this study, we evaluated two standard approaches and two new strategies in comparison with a non-treated group and a non-operated group and this enabled to evaluate and fully characterize the respective advantages and disadvantages of each strategy. The combination of a relevant animal model with a reliable and very complete follow-up protocol might serve as a model for further studies of development of a seroma prevention method.

References

1. Eroğlu E, Oral S, Ünal E, Kalayci M, Öksüz S, Tilmaz M (1996) Reducing seroma formation with fibrin glue in an animal mastectomy model, European Journal of Surgical Oncology 22: 137-139.
2. Vitug AF and Newman L A (2007) Complications in Breast Surgery, Surgical Clinics of North America 87: 431-451.
3. Salari N (2021) The Global Prevalence of Seroma After Abdominoplasty: A Systematic Review and Meta-Analysis, Aesthetic Plastic Surgery 45: 2821-2836.
4. Clough KB, Louis-Sylvestre C, Fitoussi A, Couturaud B, Nos C (2002) Donor site sequelae after autologous breast reconstruction with an extended latissimus dorsi flap. Plast Reconstr Surg 109: 1904-1911.
5. Delay E, Gounot N, Bouillot A, Zlatoff P, Rivoire M (1998) Autologous latissimus breast reconstruction: a 3-year clinical experience with 100 patients. Plast Reconstr Surg 102: 1461-1478.
6. Kottayasamy-Seenivasagam R, Gupta R, Singh G (2013) Prevention of seroma formation after axillary dissection-A comparative randomized clinical trial of three methods. Breast Journal 19: 478-484.
7. Thomson DR, Sadideen H, Furniss D (2013) Wound drainage after axillary dissection for carcinoma of the breast, Cochrane Database of Systematic Reviews 2013.
8. He X D, Guo Z H, Tian J H, Yang K H, Xie X D, (2011) Whether drainage should be used after surgery for breast cancer? A systematic review of randomized controlled trials, Medical Oncology 28.
9. Rice DC ,Morris SM, Sarr MG,Farnell MB, van-Heerden JA et al. (2000) Intraoperative Topical Tetracycline Sclerotherapy Following Mastectomy A Prospective. Randomized Trial 2000.
10. Turk E, Karagulle E, Coban G, Yildirim E, Moray G (2014) Effect of topical tetracycline on seroma formation in the lichtenstein technique: A prospective randomized study, International Surgery 99: 147-152.
11. Klima DA, Brintzenhoff RA, Trisline VB, Heniford BT, Getz S, et al. (2011) Application of Subcutaneous Talc in Hernia Repair and Wide Subcutaneous Dissection Dramatically Reduces Seroma Formation and Postoperative Wound Complications 77: 888-894.
12. Liechti R, VanD-Wall BJM, Hug U, Fritsche E, Franchi A (2022) Article Tranexamic acid use in breast surgery: a systematic review and meta-analysis. Plastic and Reconstructive Surgery 151: 949-957.
13. Kulber DA (1997) The use of fibrin sealant in the prevention of seromas. Plast Reconstr Surg 99: 842-851.
14. Johnson LN, Cusick TE, Helmer SD, Osland JS, (2005) Influence of fibrin glue on seroma formation after breast surgery, in American Journal of Surgery 2005: 319-323.
15. Benevento R (2014) The effects of low-thrombin fibrin sealant on wound serous drainage, seroma formation and length of postoperative stay in patients undergoing axillary node dissection for breast cancer: A randomized controlled trial. International Journal of Surgery 12: 1210-1215.
16. Ali SN, Gill P, Oikonomou D, Sterne GD (2010) The combination of fibrin glue and quilting reduces drainage in the extended latissimus dorsi flap donor site. Plast Reconstr Surg 125: 1615-1619.
17. Janis JE, Khansa L, Khansa I (2016) Strategies for postoperative

seroma prevention: A systematic review, Plastic and Reconstructive Surgery 138: 240-252.

18. Matarasso A, Matarasso DM, Matarasso EJ (20) Abdominoplasty: Classic principles and technique, Clinics in Plastic Surgery 41: 655-672.

19. VanBemmel AJM, VanDe-Velde CJH, Schmitz RF, Liefers GJ (2011) Prevention of seroma formation after axillary dissection in breast cancer: A systematic review,European Journal of Surgical Oncology 37: 829-835.

20. Sajid MS, Hutson KH, Rapisarda IH, Bonomi R (2013) Fibrin glue instillation under skin flaps to prevent seroma-related morbidity following breast and axillary surgery,Cochrane Database of Systematic Reviews 2013: CD009557.

21. Nasr MW, Jabbour SF, Mhawe RI, Elkhoury JS, Sleilati FH (2016) Effect of Tissue Adhesives on Seroma Incidence after Abdominoplasty: A Systematic Review and Meta-Analysis. Aesthetic Surgery Journal 36: 450-458.

22. Lindsey WH, Masterson TM, Spotnitz WD, Wilhelm MC, Morgan RF (1990) Seroma prevention using fibrin glue in a rat mastectomy model. Arch Surg 125: 305-307.

23. Harada RN, Pressler VM, McNamara JJ (1992) Fibrin glue reduces seroma formation in the rat after mastectomy. Surg Gynecol Obstet 175: 450-454.

24. Chung TL, Holton LH, Goldberg NH, Silverman RP (2006) Seroma prevention using Mytilus edulis protein in a rat mastectomy model, Breast Journal 12: 442-445.

25. Choi MS, Kim HK, Kim WS, Bae TH, Kim MK (2012) A comparison of triamcinolone acetonide and fibrin glue for seroma prevention in a rat mastectomy model. Ann Plast Surg 69: 209-212.

26. Hurwitz ZM, Ignotz RA, Rowin C, Freniere BB, Lalikos JF, et al. (2015) Seroma formation in rat latissimus dorsi resection in the presence of biologics: The role of quilting. Ann Plast Surg 75: 338-342.

27. Mücke T, Fichter M, Schmidt LH, Mitchell DH, Wolff KD, et al. (2017) Indocyanine green videoangiography assisted prediction of flap necrosis in the rat epigastric flap using the flow® 800 tool. Microsurgery 37: 235-242.

28. Holm C, Mayr M, Höfter E, Becker A, Pfeiffer UJ,et al. (2002) Intraoperative evaluation of skin-flap viability using laser-induced fluorescence of indocyanine green. Br J Plast Surg 55: 635-644.

29. Matsui A (2009) Real-time intraoperative near-infrared fluorescence angiography for perforator identification and flap design. Plastic and Reconstructive Surgery 123: 125e-127e.

30. Haslik W (2014) Indocyanine green video angiography predicts outcome of extravasation injuries. PLoS One 9: e103649.

31. Kim JS (2020) Effect of Collagen-Enhanced Fibrin Sealant on Seroma Formation in a Rat Mastectomy Model. Journal of Wound Management and Research 16: 137-143.

32. Seretis K, Goulis D, Demiri EC, Lykoudis EG (2017) Prevention of seroma formation following abdominoplasty: A systematic review and meta-analysis. Aesthet Surg J 37: 316-323.

33. Gisquet H, Delay E, Paradol PO, Toussoun PO (2010) Delaporte Prevention of by quilting suture after harvesting latissimus dorsi flap. The 'Chippendale' technic. Annales de Chirurgie Plastique Esthetique 55: 97-103.

34. Bercial ME, Neto MS, Calil JA, Rossetto LA, Ferreira LM (2012) Suction Drains, Quilting Sutures, and Fibrin Sealant in the Prevention of Seroma Formation in Abdominoplasty: Which is the Best Strategy?. Aesthetic Plast Surg 36: 370-373.

35. Nahas FX, Ferreira LM, Ghelfond C (2007) Does quilting suture prevent seroma in abdominoplasty?. Plast Reconstr Surg 119: 1060-1064.

36. Pollock H, Pollock T (2000) Techniques in Cosmetic Surgery Progressive Tension Sutures: A Technique to Reduce Local Complications in Abdominoplasty. Plast Reconstr Surg 105: 2583-2588.

37. Andrades P (2007) Progressive tension sutures in the prevention of postabdominoplasty seroma: A prospective, randomized, double-blind clinical trial. Plast Reconstr Surg 120: 935-946.

38. Dancey AL, Cheema M,Thomas SS (2010) A prospective randomized trial of the efficacy of marginal quilting sutures and fibrin sealant in reducing the incidence of seromas in the extended latissimus dorsi donor site. Plast Reconstr Surg 125: 1309-1317.

39. Carless PA, Henry DA (2006) Systematic review and meta-analysis of the use of fibrin sealant to prevent seroma formation after breast cancer surgery. British Journal of Surgery 93: 810-819.

40. Dinsmore RC, Harris JA, Gustafson RJ (2000) Effect of Fibrin Glue on Lymphatic Drainage after Modified Radical Mastectomy: A Prospective Randomized Trial. Am Surg 66: 982-985.

41. Miri-Bonjar MR, Maghsoudi H, Samnia R, Saleh P, Parsafar F (2012) Efficacy of Fibrin Glue on Seroma Formation after Breast Surgery. Int J Breast Cancer 2012: 643132.

42. Walgenbach KJ, Bannasch H, Kalthoff S, Rubin JP (2012) Randomized, prospective study of TissuGlu® surgical adhesive in the management of wound drainage following abdominoplasty. Aesthetic Plastic Surgery 36: 491-496.

43. Duarte AP, Coelho JF, Bordado JC, Cidade MT, Gil MH (2012) Surgical adhesives: Systematic review of the main types and development forecast. Progress in Polymer Science 37: 1031-1050.

44. Bouten PJM (2014) The chemistry of tissue adhesive materials. Progress in Polymer Science Elsevier Ltd 39: 1375-1405.

45. Vakalopoulos KA (2013) Tissue adhesives in gastrointestinal anastomosis: A systematic review. Journal of Surgical Research 180: 290-300.

46. Toriumi DM, Raslan WF, Friedman M, Eugene M (1990) Histotoxicity of Cyanoacrylate Tissue Adhesives A Comparative Study. Arch Otolaryngol Head Neck Surg 116: 546-550.

47. Navarro-Triviño FJ, Cuenca-Manteca J, Ruiz-Villaverde R (2020) Allergic contact dermatitis with systemic symptoms caused by VenaSeal. Contact Dermatitis 82: 185-187.

48. Mestieri LB, Saska S, Carrodeguas RG, Gaspar AMM (2012) Evaluation of n-butyl cyanoacrylate adhesive in rat subcutaneous tissue. Dermatologic Surgery 38: 767-771.

49. Ibrahim SR, Ward PJ (2020) Tissue Adhesives for Hernia Mesh Fixation: A Literature Review. Cureus 12: e10494.

50. Foresta E (2015) Use of N-Butyl-2-Cyanoacrylate (Glubran2®) in Fractures of Orbital-Maxillo-Zygomatic Complex. J Maxillofac Oral Surg 14: 761-764.

51. Yoon N, Shah A, Couldwell WT, Kalani MYS, Park MS (2018) Preoperative embolization of skull base meningiomas: Current indications, techniques, and pearls for complication avoidance. Neurosurg Focus 44.

52. Harada T, Fujita A, Sakata J, Kohta M, Kohmura E (2021) Endovascular Internal Trapping by Low-Concentration N-butyl-2-Cyanoacrylate for a Ruptured Giant Common Carotid Artery Pseudoaneurysm. Vasc Endovascular Surg 55: 81-85.

53. Lam YL, DeMaeseneer M, Lawson J, De-Borst GJ, Boersma D (2017) Expert review on the VenaSeal® system for endovenous cyano-acrylate adhesive ablation of incompetent saphenous trunks in patients with varicose veins. Expert Review of Medical Devices, Taylor and Francis Ltd 14: 755762.

54. Al-Masri M (2021) Effectiveness of Cyanoacrylate in Reducing Seroma Formation in Breast Cancer Patients Post-Axillary Dissection: A Randomized Controlled Trial. Front Oncol 10: 580861.

55. Vasileiadou K, Kosmidis C, Anthimidis G, Miliaras S, Kostopoulos I, et al. (2017) Cyanoacrylate Adhesive Reduces Seroma Production After Modified Radical Mastectomy or Quadrantectomy With Lymph Node Dissection-A Prospective Randomized Clinical Trial. Clin Breast Cancer 17: 595-600.

56. Lee JH, Kim HL, Lee MH, Taguchi H, Hyon SH, et al. (2011) Antimicrobial effect of medical adhesive composed of aldehyded dextran and ε-poly (L-lysine). J Microbiol Biotechnol 21: 1199-1202.

57. Lee DH, Lee DH, Ko W (2020) Hemostatic materials in non-variceal upper gastrointestinal hemorrhage. International Journal of Gastrointestinal Intervention 9: 1-3.

58. Shin J (2021) Efficacy of a novel hemostatic adhesive powder in patients with upper gastrointestinal tumor bleeding. BMC Gastroenterol 21: 40.

59. Cha B, Lee D, Shin J, Park JS, Suk-Kwon G, et al. (2022) Hemostatic efficacy and safety of the hemostatic powder UI-EWD in patients with lower gastrointestinal bleeding. BMC Gastroenterol 22: 170.

60. Takagi K (2013) Novel powdered anti-adhesion material: Preventing postoperative intra-abdominal adhesions in a rat model. Int J Med Sci 10: 467-474.

61. Takai F (2020) Management of retrosternal adhesion after median sternotomy by controlling degradation speed of a dextran and ε-poly (l-lysine)-based biocompatible glue. Gen Thorac Cardiovasc Surg 68: 793-800.

62. T Kamitani, H Masumoto, H Kotani, T Ikeda, SH Hyon, et al. (2013) Prevention of retrosternal adhesion by novel biocompatible glue derived from food additives. Journal of Thoracic and Cardiovascular Surgery 146: 1232-1238.

63. Yang R (2022) Injectable polylysine and dextran hydrogels with robust antibacterial and ROS-scavenging activity for wound healing. Int J Biol Macromol 223: 950-960.

64. Hyon W, Hyon SH, Matsumura K (2022) Evaluation of the optimal dose for maximizing the anti-adhesion performance of a self-degradable dextran-based material. Carbohydrate Polymer Technologies and Applications 4: 100255.